ACS APPLIED MATERIALS & INTERFACES

Research Article

www.acsami.org

High-Performance Flexible Ultraviolet (UV) Phototransistor Using Hybrid Channel of Vertical ZnO Nanorods and Graphene

Vinh Quang Dang,[†] Tran Quang Trung,[†] Le Thai Duy,[†] Bo-Yeong Kim,[‡] Saqib Siddiqui,[†] Wonil Lee,[†] and Nae-Eung Lee*[,†,‡,§]

[†]School of Advanced Materials Science & Engineering, Sungkyunkwan University, Suwon, Kyunggi-do 440-746, Korea

[‡]SKKU Advanced Institute of Nanotechnology (SAINT), Sungkyunkwan University, Suwon, Kyunggi-do 440-746, Korea

[§]Samsung Advanced Institute for Health Sciences & Technology (SAIHST), Sungkyunkwan University, Suwon, Kyunggi-do 440-746, Korea

Supporting Information

ABSTRACT: A flexible ultraviolet (UV) photodetector based on ZnO nanorods (NRs) as nanostructure sensing materials integrated into a graphene (Gr) field-effect transistor (FET) platform is investigated with high performance. Based on the negative shift of the Dirac point (V_{Dirac}) in the transfer characteristics of a phototransistor, high-photovoltage responsivity (R_V) is calculated with a maximum value of 3×10^8 V W^{-1}. The peak response at a wavelength of ~365 nm indicated excellent selectivity to UV light. The phototransistor also allowed investigation of the photocurrent responsivity (R_I) and photoconductive gain (G) at various gate voltages, with maximum values of 2.5×10^6 A W^{-1} and 8.3×10^6, respectively, at a gate bias of 5 V. The UV response under bending conditions was virtually unaffected and was unchanged after 10 000 bending cycles at a bending radius of 12 mm, subject to a strain of 0.5%. The attributes of high stability, selectivity, and sensitivity of this flexible UV photodetector based on a ZnO NRs/Gr hybrid FET indicate promising potential for future flexible optoelectronic devices.

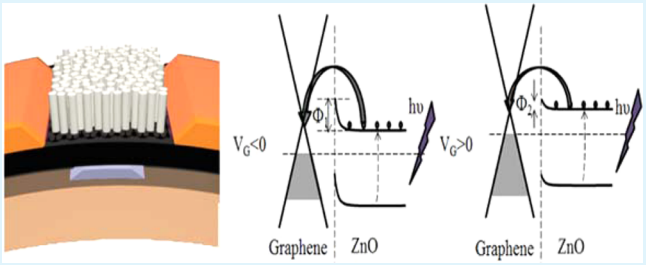

KEYWORDS: *ZnO nanorods, graphene, field-effect transistor, ultraviolet photodetector, flexible*

INTRODUCTION

With the advent of smart wearable electronics, sensing devices are emerging with the potential to play critical roles in the monitoring of humans and their surrounding environment.[1,2] For the realization of smart wearable electronics for pervasive computing, a multitude of sensors must be integrated into various formats of wearable systems,[2−4] including clothing, watches, glasses, rings, contact lenses, badges, electronic skin, and patches. In order to integrate the sensing devices into wearable formats that require mechanical deformability and transformability (such as clothing, contact lenses, or body patches), flexible or stretchable sensing devices have been attracting rapidly increasing attention. Flexible sensors with simple processing, low cost, lightweight, shock resistance, durability, and flexibility[5,6] can create new possibilities for on-body wearable systems.[7] In particular, flexible photodetectors for ultraviolet (UV), visible, or infrared (IR) light are of great technological interest for the monitoring of humans and their surrounding environment in a new and unobtrusive way, because they may overcome the limits of rigid photodetectors.[8] Flexible visible and IR photodetectors were demonstrated to detect the pulse rate in combination with light-emitting diodes.[9] Among photodetectors, UV detectors are attracting interest for the detection of UV during daily activities; for example, UV photodetectors can be used to monitor the level of UV intensity on human skin.[10]

For highly sensitive UV photodetectors on rigid substrates, ZnO nanostructures (including quantum dots,[11] nanotetrapods,[12] nanowires (NWs),[13,14] and nanorods (NRs)[15−17]) have been used primarily. In particular, ZnO NRs have been extensively investigated for UV photodetectors because they have photoabsorption in the UV range[18,19] and high exciton binding energy of 60 meV,[12,20] and they are relatively easy to synthesize. Although the low photocurrent of single ZnO NW photodetectors results in low responsivity and limits their practical applications,[21] ZnO NR photodetectors have exhibited a fast photoresponse time (<0.4 ms)[14] and extremely high sensitivity to UV light exposure.[13]

For the realization of flexible UV photodetectors based on ZnO nanostructures, integration of ZnO nanostructures into a flexible substrate is critically important. Flexible integrated ZnO NW photodetectors showed the same photocurrent as UV photodetectors built on rigid substrates and their performance in the UV region exhibited near invariance under flexure.[18] Although ZnO NW UV sensors on a polyethylene tereph-

Received: April 1, 2015
Accepted: May 5, 2015
Published: May 5, 2015

DOI: 10.1021/acsami.5b02834
ACS Appl. Mater. Interfaces 2015, 7, 11032−11040

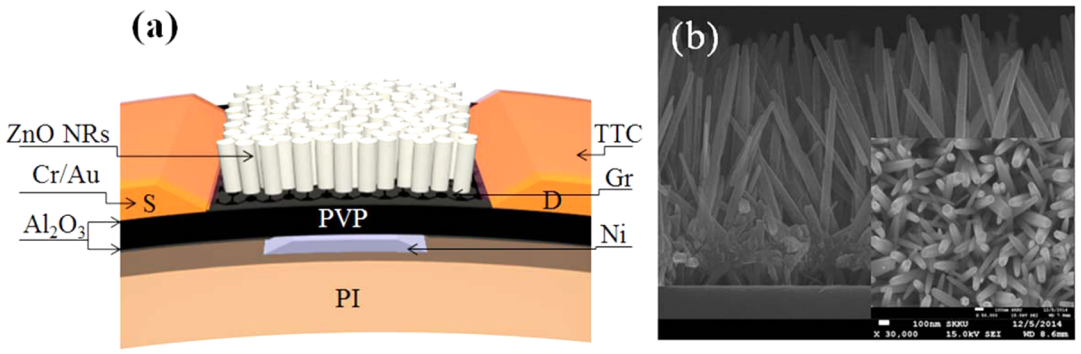

Figure 1. (a) Cross-sectional schematic of the hybrid FET photodetector on a flexible polyimide substrate. (b) Cross-sectional FE-SEM image of ZnO NRs grown on the Gr channel on a flexible polyimide substrate (inset shows a top-view FE-SEM image of the ZnO NRs).

thalate (PET) substrate presented high sensitivity and fast response speed under UV light exposure, a nonsmooth signal current was observed during UV exposure.[22] In addition, because the contact between metal electrodes and ZnO NWs was weak, the performance of ZnO NW devices was easily degraded after high cyclic bending.[23] Furthermore, to enhance the photocurrent, the number of ZnO NWs must be increased, but the integration of many ZnO NWs on a flexible substrate and the collective electrical contacts to them are limited. In contrast, ZnO NRs are promising candidates for flexible[24−26] and stretchable[27] UV photodetectors, because they exhibit not only excellent UV absorption and high elastic modulus, but can also be fabricated with a simple synthesis method of a hydrothermal process that is low-cost, compatible with low temperatures, easy to control and fast. Specifically, one way of achieving a flexible ZnO NR photodetector is to integrate ZnO NRs with flexible transport channels in a flexible field-effect transistor (FET) platform, which may enable the generation of a flexible UV photodetector.

One of the candidates for a flexible channel material in phototransistors is two-dimensional graphene (Gr), which has high mobility (up to $\sim 10^6$ cm^{-2} V^{-1} s^{-1} at room temperature),[28−30] high mechanical flexibility,[31] and is an excellent template for the vertical growth of dense ZnO NRs.[32] Moreover, Gr FETs exhibit ambipolar behavior in transfer characteristics,[33] which enables investigation of the charge transfer mechanism between the Gr channel and ZnO NRs. Recently, rigid ZnO NRs/Gr hybrid UV sensors have been investigated.[34] For example, the Schottky junction UV photodetector with a coating of a free-standing ZnO NR array on a single layer of Gr exhibited high sensitivity to UV light exposure, good reproducibility, and fast response speed.[35] The reported responsivities of UV sensors are ~22.7 A W^{-1} for *in situ* solution-grown ZnO NR/Gr heterostructure on a silicon substrate[36] and 1.6 A W^{-1} per volt for vertically aligned ZnO micro/nanowires on Gr UV photodetectors.[20] A higher responsivity (>10^4 A W^{-1}) was achieved with a ZnO NW device using a transparent Gr top electrode,[37] whereas this value was only 86.0 A W^{-1} for the ZnO NR MSM photodetector with Ag/Au contact electrodes.[38] Most of the rigid UV photodetectors based on a hybrid structure between Gr and ZnO NRs cannot be directly converted to flexible UV photodetectors, because the processes and components must be adapted for mechanical flexibility. Furthermore, most of the ZnO NR/Gr hybrid UV photodetectors used a Schottky diode,[35] photoconductor,[20,36,37] or a core−shell structure of the detector,[39] which makes it difficult to extract the sensing mechanism in detail. Therefore, a clear understanding of the UV photoresponse mechanism and design of flexible UV photodetectors for practical applications have been the biggest challenges to date. To overcome those problems, flexible FET photodetectors with ZnO NRs on a flexible Gr channel are an interesting option.

Here, we demonstrate a transistor device that combines highly UV-absorbing ZnO NRs and Gr channels as a charge transport layer of the UV photodetector on a flexible polyimide (PI) substrate. In this case, Gr also works as a template for the growth of ZnO NRs and allows their integration into a flexible format. ZnO NRs on Gr are mechanically stable and are formed with a strong interaction at the atomic/molecular level.[32] Indeed, the C atoms of Gr directly bind to the Zn atoms of ZnO NRs at the ZnO NRs/Gr interface and the destabilization energy of ZnO−Gr binding is low, indicating that ZnO has a stable bond with Gr.[32] The dependence of the photocurrent on the excitation UV intensity at different gate voltage and photovoltage is investigated. The negative shifts of the Dirac point in the transfer characteristics under UV exposure provide an in-depth understanding of the photoresponse mechanism in ZnO NRs, coupled with Gr transport channels. The average electron concentration transferred from ZnO NRs to Gr is calculated as 6×10^{12} electrons per mW cm^{-2}. The maximum response around a wavelength of 365 nm affirmed the selective property of our device. The flexible ZnO NRs/Gr hybrid FET photodetector shows that the responsivity (R_I) and photoconductive gain (G) at a positive gate voltage are higher than those at a negative voltage. The maximum values of R_I and G are 2.5×10^6 A W^{-1} and 8.3×10^6, respectively, at a gate bias of 5 V. Investigation of the photoresponse under strain showed high stability after cyclic bending of 10 000 cycles at a strain of 0.5% under a bending radius of 12 mm. The successful fabrication of a flexible UV photodetector based on ZnO NRs/Gr hybrid FET has promising potential for wearable or curvilinear devices and opens up a broad range of real-life applications.

RESULTS AND DISCUSSION

A flexible hybrid FET photodetector was fabricated on PI substrates with a sandwich dielectric of 400 nm-thick polyvinylpyrrolidone (PVP) between two bottom and top layers of 20 nm-thick Al_2O_3 and 60 nm-thick Ni gate electrodes. The sensing antenna of ZnO NRs was vertically grown on a Gr transport layer. Cr/Au layers of 5 nm/50 nm thicknesses were used as source-drain electrodes. The cross-sectional view of the hybrid FET photodetector is schematically depicted in Figure

DOI: 10.1021/acsami.5b02834
ACS Appl. Mater. Interfaces 2015, 7, 11032−11040

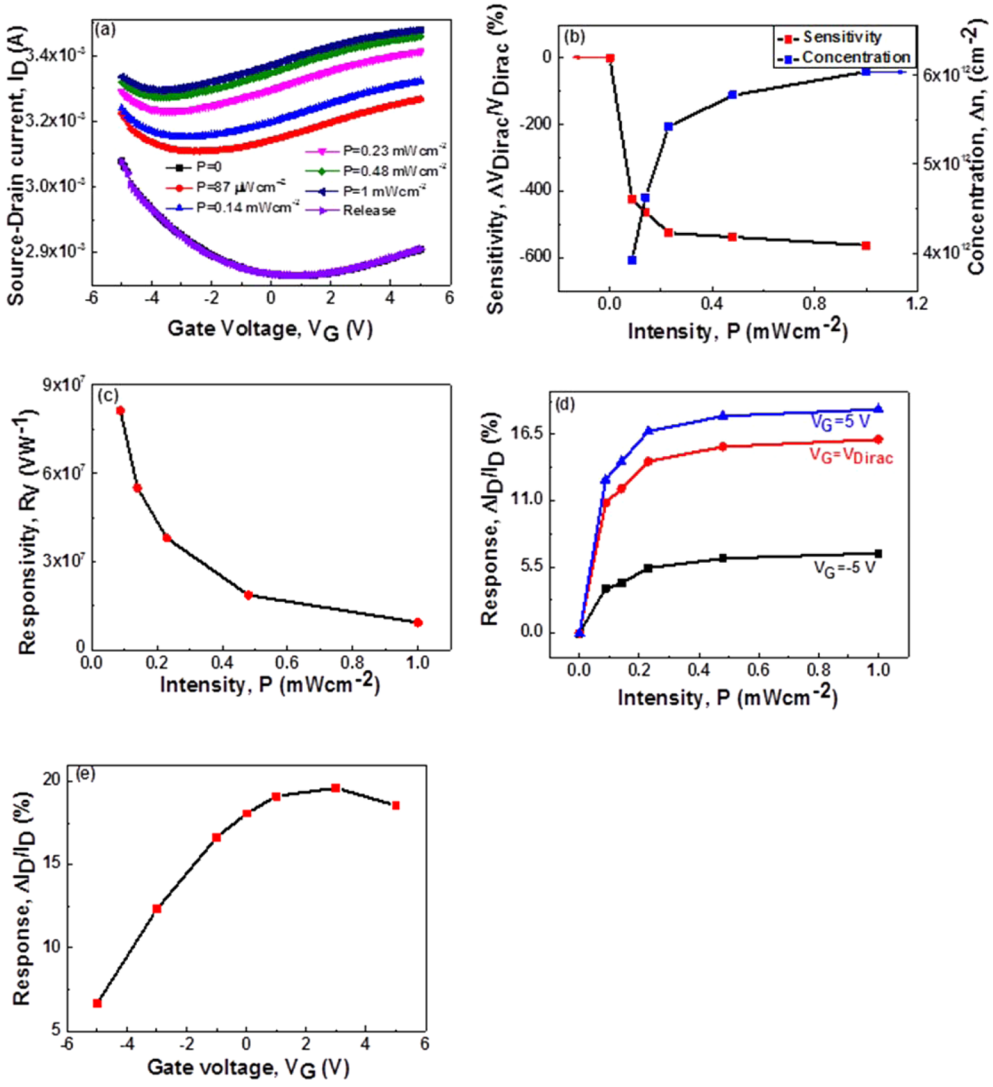

Figure 2. (a) Transfer characteristics of the ZnO NR/Gr hybrid FET photodetector. The gate voltage (V_G) was varied at a source−drain voltage (V_D) of 1 V. (b) Sensitivity in Dirac point shifts ($\Delta V_{Dirac}/V_{Dirac}$) and electron concentration transfer from ZnO NRs to Gr (Δn) in a hybrid FET phototransistor under varying UV intensity. (c) Responsivity of photovoltage (R_V) at various UV intensities. (d) Photocurrent response ($\Delta I_D/I_D$) of the devices at different V_G, measured as a function of UV intensity. (e) Dependence of response on the V_G at a fixed incident illumination intensity of 1 mW cm^{-2}.

1a. A key aspect of the hybrid FET photodetector fabrication is to achieve the bottom-gated configuration for integration of ZnO NRs on the Gr channel. Growth process of ZnO NRs on Gr was similar to that reported previously.[32,40,41] The process for fabricating the bottom-gated FET device is described in more detail in the Methods section. Figure 1b shows the cross-sectional FE-SEM image of ZnO NRs on a Gr layer, and the top view of it is shown in the inset in Figure 1b. The average length and diameter of ZnO NRs are ∼2 μm and a few tens of nanometers, respectively. The size of ZnO NRs affects the performance of the UV detector. If the length of the rods is too short, the surface area absorbing UV radiation becomes small, resulting in low response. However, ZnO NRs are easily overlapped together, deformed, or even broken if the length of the rods is too long. In this case, the length of ∼2 μm was found to be reasonable for our photodetector, because of the limit of growth conditions, as well as the device fabrication processes. The hexagonal morphology of ZnO NRs is clearly observed in the inset of Figure 1b. The single-crystalline nature of ZnO NRs, as well as the interface between ZnO NRs and Gr, were clearly verified in the previous works.[32,40]

To study the performance of the flexible ZnO NRs/Gr hybrid FET photodetector, the transfer characteristics were measured at a wavelength of 365 nm with intensity ranging from 87 μW cm^{-2} to 2 mW cm^{-2}, and the drain current (I_D) was plotted as a function of the gate bias voltage (V_G) (see Figure 2a, as well as Figure S1a in the Supporting Information). The Dirac point (V_{Dirac}) was shifted to the negative direction and the minimum currents ($I_{D,min}$) at V_{Dirac} increased with the increase in UV light intensity. Here, V_{Dirac} is the gate voltage value at the minimum drain current I_D in the transfer curve. The two curves of "p = 0" and "release" overlap together, which proves a good recovery characteristics of our device. The shift of the transfer characteristics was attributed to the accumulation of electrons in the Gr transport channel that were transferred from ZnO NRs under UV light illumination.

Based on the shift of V_{Dirac} in the transfer characteristics, the sensitivity was plotted as a function of UV intensity (Figure 2b). The sensitivity, which is defined as the ratio of the shift of

DOI: 10.1021/acsami.5b02834
ACS Appl. Mater. Interfaces 2015, 7, 11032−11040

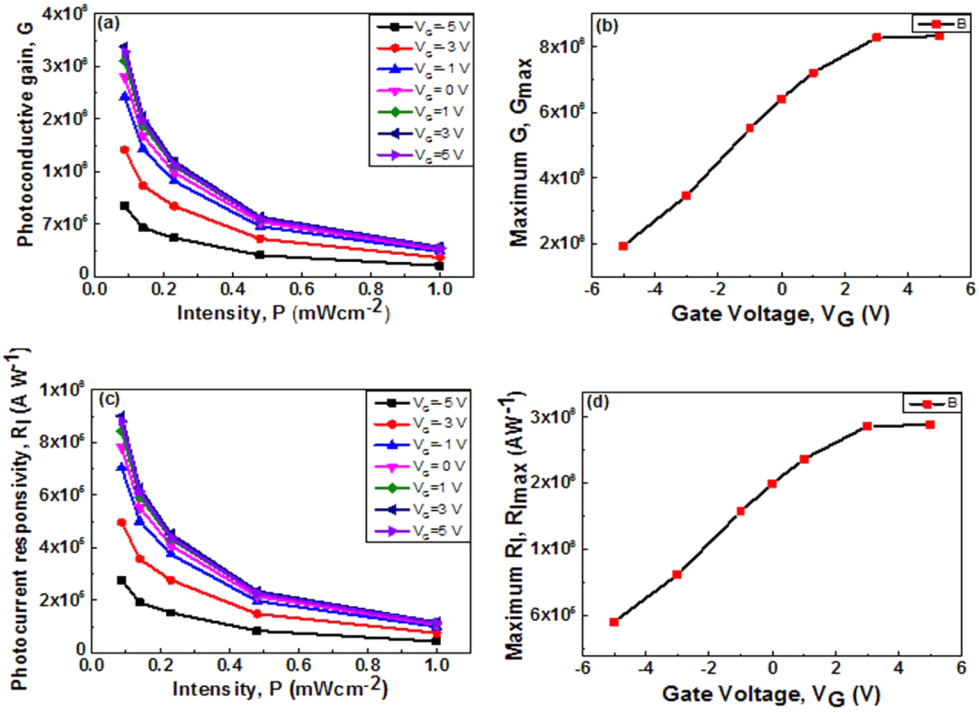

Figure 3. (a) Photoconductive gain (G) and (c) photocurrent responsivity (R_I), as a function of UV intensity at various V_G values. (b) Maximum G and (d) R_I of the ZnO NR/Gr hybrid FET under different V_G values.

V_{Dirac} under UV exposure to V_{Dirac} under dark conditions ($\Delta V_{Dirac}/V_{Dirac}$), increased with the increase in the UV intensity and nearly reached a saturated state at high UV intensity. This result was attributed to the carrier transfer mechanism that is discussed in more detail below. The electron concentrations transferred from ZnO NRs to the Gr channel under UV radiation were calculated from the shift of V_{Dirac}:[42,43]

$$\Delta n = \frac{C_0|V_{Dirac} - V_{Dirac,0}|}{e} \quad (1)$$

where C_0 is the capacitance of the gate dielectric per unit area. For a sandwich dielectric Al_2O_3/PVP/Al_2O_3 (20 nm/400 nm/20 nm), the measured value of C_0 was ~198 nF/cm^2. The dependence of transferring electron concentration on UV light intensity is also presented in Figure 2b. The higher the illuminating UV intensity, the larger the electron concentration transferred from ZnO NRs to the Gr. At a UV intensity of 1 mW cm^{-2}, this value is $\sim 6 \times 10^{12}$ electrons/cm^2.

Interestingly, our FET structure exhibits high photovoltage responsivity (R_V) based on the shift of V_{Dirac}. R_V, which is an important parameter in a photodetector, is used to characterize the generated photovoltage (V_{ph}) per incident UV intensity (P) at a certain wavelength, $R_V = (V_{ph}/P)$.[44] Figure 2c illustrates R_V with exposure to 365 nm UV wavelengths of different intensities. A decrease in R_V was observed with an increase in UV intensity. From the fitting curve of the dependence of R_V on the UV light intensity (see Figure S1b in the Supporting Information), as the UV intensity approached zero ($P \rightarrow 0$), the R_V values of the flexible ZnO NRs/Gr hybrid channel FET photodetector reached a maximum of 3×10^8 V W^{-1}.

In addition to the negative shift in V_{Dirac}, the I_D value at various gate voltages also increases under UV light exposure. The response is described as the ratio of the photocurrent (ΔI_D) to the dark current (I_D),

$$\frac{\Delta I_D}{I_D} = \frac{I_{ph} - I_D}{I_D}$$

where I_{ph} is the change of current under UV light radiation. Specifically, with the transistor structure, the photocurrent response can be studied under different gate voltages. Here, we plotted the relationship between the response and UV intensity at negative V_{Dirac} and positive gate voltage (see Figure 2d, as well as Figure S2 in the Supporting Information). With the same UV intensity range, the photoresponse became higher at a positive V_G and lower at a negative V_G. This result is explained by the internal electric field that came from the applied V_G. It was already known that the photoresponse is caused by transfer of electrons from ZnO NRs to Gr under UV light exposure. The positive back gate voltage formed an internal electric field that caused a drift of electrons from ZnO NRs to Gr. Consequently, the transferred electron concentration was enhanced. In contrast, the internal electric field caused by a negative V_G restrained the drift of electrons from ZnO NRs to Gr. That is why the UV response of the flexible hybrid phototransistor under positive V_G was higher than that under negative V_G. Figure 2e shows the dependence of the photocurrent response on V_G at the same UV intensity of 1 mW cm^{-2}. The response was increased with the change from negative to positive gate bias; however, it decreased at a high positive gate voltage of 5 V. This increase in response is related to the enhancement of the number of transferrable electrons from ZnO NRs to Gr, which will be discussed in more detail later in this work, in connection with Figure 5.

In order to characterize the performance of a UV photodetector, the photocurrent responsivity (R_I) and photoconductive gain (G) were investigated. R_I of the photon detector was defined as the ratio of photocurrent to the UV light intensity,[37,45]

DOI: 10.1021/acsami.5b02834
ACS Appl. Mater. Interfaces 2015, 7, 11032−11040

Table 1. Comparison of Responsivity of the ZnO Nanostructure-Based Photodetectors

active layer (channel)	structure	wavelength (nm)	gate bias (V)	responsivity (A W^{-1})	ref
ZnO wire	MSM	372		4.5×10^4	59
n-ZnO/*p*-Si	photodiodes	365		0.63	60
mechanically exfoliated SLG/ZnO QDs	FET	325	0	10^4	47
CVD Gr/ZnO NR array	Schottky diode	365		113	35
ZnO/Ag NW/ZnO	composite	365		2.4	61
CVD Gr/vertically aligned ZnO wires	photoconductor	365		13.8	20
ZnO NRs/CVD Gr	FET	365	0	3×10^5	34
ZnO NRs/CVD Gr	FET	365	0	1.89×10^6	this work
	(flexible)	365	5	2.5×10^6	this work

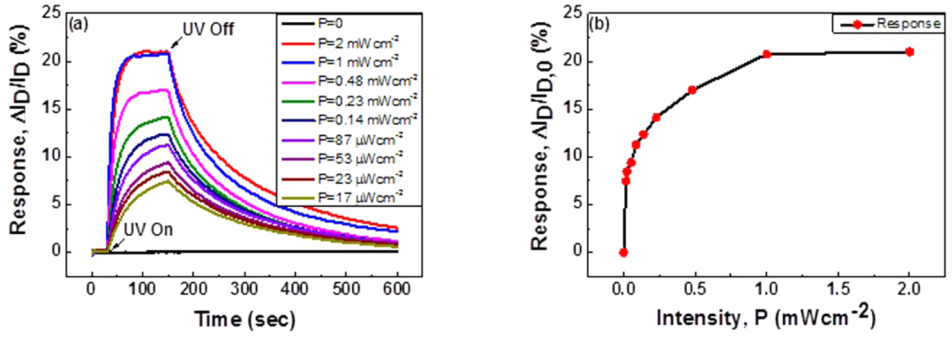

Figure 4. (a) Time-dependent responses of the flexible ZnO NR/Gr hybrid FET photodetector measured as a function of UV intensities at a fixed V_G of 0 V and V_D of 1 V. (b) Responses of the ZnO NP/Gr hybrid FET photodetector at various UV intensities.

$$R_I = \frac{\Delta I_D}{P} = \frac{I_{ph} - I_D}{P}$$

whereas G was described as the number of detected carriers per absorbed photon and calculated by the ratio between the number of electrons collected per unit time and the number of absorbed photon per unit time,[37,46,47]

$$G = \frac{N_e}{N_{ph}} = \frac{I_{ph}}{P} \times \frac{h\nu}{e\lambda}$$

where e is the elementary charge and $h\nu$ is the photon energy of incident UV light. Figures 3a and 3c display the UV intensity dependence of G and R_I, respectively, at various V_G. At low UV intensity, an extreme decrease in G was observed (Figure 3a), whereas G reached saturation at high UV intensity. With increasing UV intensity, G is decreased because of the oxygen-related hole trapping states. Indeed, the reduction of G at low light intensities is consistent with charge carrier photogeneration efficiency, which is proportional to the absorbed photon flux.[37,46] As the excitation UV intensity increases, more and more electron−hole pairs are generated. After separating, the photoholes migrate to the ZnO NR surface and are trapped at the surface,[47] until they fill the entire surface state. The trapped photoholes occupying the surface state modify the potential profile and reduce the depletion region near the ZnO NR surface.[37] This causes a change in the conducting surface of ZnO, which is the key mechanism responsible for G.[37,46] At a certain UV intensity, when all of the surface states are filled, the extra holes that are separated from photogenerated electron−hole pairs immediately recombine with unpaired electrons instead of moving to the surface states.[47] Therefore, G reaches a saturated state at high UV intensities. Remarkably, in agreement with the theory,[46,47] the experimental data of UV excitation intensity-dependent G (Figure 3a) could be fitted by the reciprocal function,

$$G = \frac{a}{1 + (bP)^n}$$

where a and b are constants and n is a phenomenological fitting parameter ($n \approx 1$) (see Figure S3a in the Supporting Information). From the fitting curves, the maximum G (G_{max}) value of a flexible ZnO NRs/Gr hybrid phototransistor, calculated at very low excitation intensity ($P \rightarrow 0$), was plotted as a function of V_G (Figure 3b). At V_G values from −5 V to +3 V, G_{max} exhibited an almost-linear increase, from 1.94×10^6 to 8.3×10^6. However, G_{max} seemed to be nearly invariant at V_G = 5 V, because of the leakage current. Indeed, the potential between the gate electrode and the drain electrode became very large at a high positive V_G. Hence, the leakage current in the dielectric increased.

To estimate the maximum value of R_I (R_{Imax}), the reduction of R_I with UV intensity at different V_G (Figure 3c) was also fitted by the reciprocal function (see Figure S3b in the Supporting Information). As P approaches zero ($P \rightarrow 0$), R_I of the ZnO NRs/Gr hybrid photodetector reached the maximum value. The dependence of R_{Imax} on V_G is presented in Figure 3d. R_{Imax} at positive V_G was higher than that at negative V_G. At a high positive V_G, R_{Imax} displayed an almost-saturated state and reached 2.5×10^6 A W^{-1} at V_G = 5 V. The responsivity in our work was compared with other reports in Table 1.

The increase in I_D under UV light exposure was also verified by time-dependent measurements of the UV response. The time-resolved photoresponse of the flexible ZnO NRs/Gr hybrid FET photodetector at various UV intensities is depicted in Figure 4a; the results show an increasing photoresponse with increasing UV light intensity. Based on the time-dependent spectra (Figure 4a), the relationship between photoresponse and UV intensities was plotted in Figure 4b. A rapid increase in photoresponse was observed with an increase in UV intensity, because the concentration of the photogenerated electron−hole pairs was proportional to the absorbed flux.[37,46] However, at

DOI: 10.1021/acsami.5b02834
ACS Appl. Mater. Interfaces 2015, 7, 11032−11040

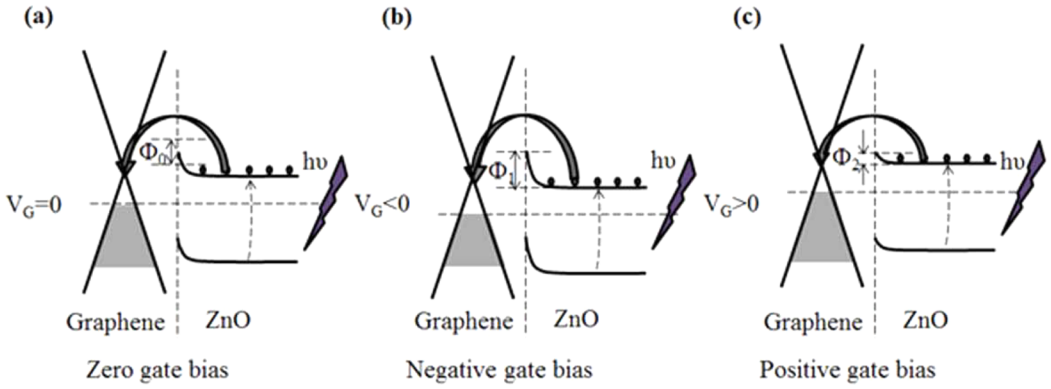

Figure 5. Energy diagrams of ZnO and Gr at (a) zero bias, (b) negative V_G, and (c) positive V_G.

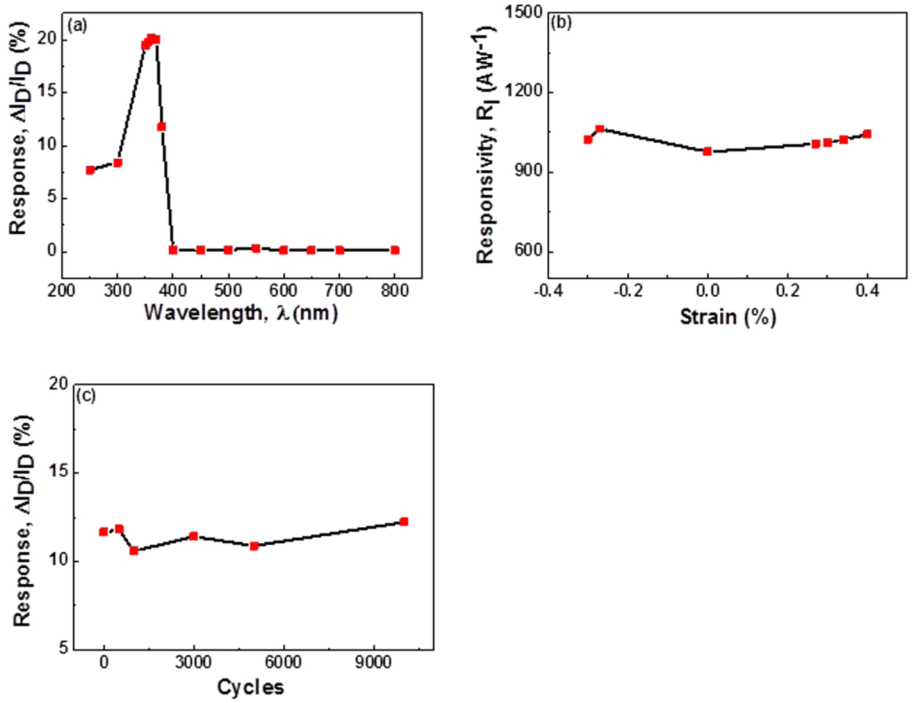

Figure 6. (a) Photocurrent response ($\Delta I_D/I_D$) of flexible ZnO NRs/Gr hybrid FET photodetector at different wavelengths. (b) Current responsivity (R_I) of flexible ZnO NRs/Gr hybrid FET photodetector under different strain conditions, from a compressive strain of 0.3% to a tensile strain of 0.4% at a wavelength of 365 nm. (c) Photocurrent response ($\Delta I_D/I_D$) of flexible ZnO NRs/Gr hybrid FET photodetector before and after cyclic bending up to 10 000 cycles at the strain of 0.5% (bending radius of 12 mm). During measurements of photoresponse, V_G and V_D were fixed at 0 and 1 V, respectively.

high UV intensities, the photoresponse reached an almost-saturated state, because of the balance between recombination and the generation of electron−hole pairs under UV radiation.[47] More importantly, our device with the encapsulation of source and drain electrodes exhibited good reproducibility and stability. The sensing performance showed very little change after numerous repetitions of switching between UV-on and UV-off states (see Figure S4 in the Supporting Information) and stable responses after long-term storage in the air.

Generally, based on the operational principles, the photodetector can be classified into two categories: a photon detector or a thermal detector.[44] Photon detectors or quantum detectors are based on semiconductors in which electron−hole pairs are generated by the absorbed photon, whereas thermal detectors convert incident light into heat within the sensing material, which leads to an electrical signal change.[44] For UV photodetectors based on a hybrid structure between Gr and a wide-bandgap ZnO NR, photon detection plays a dominant role. ZnO NRs absorb UV light to generate electron−hole pairs and form the photocurrent after efficient charge separation and transfer of electrons to Gr.

The sensing mechanism of UV photodetectors based on ZnO NRs has been extensively studied.[13,46,48−51] However, very few reports have presented the photoresponse mechanism of UV sensors based on a hybrid channel between ZnO NRs and Gr. For the FET structure, the sensing mechanism of the photodetector of ZnO NRs/Gr was fully explained in our previous report.[34] Here, we focused on explaining the dependence of the response, responsivity and photoconductive gain on gate bias. Indeed, ZnO NRs and Gr have different Fermi levels and the equilibrium state will be reached upon contact between ZnO NRs and Gr; therefore, a new quasi-Fermi level is formed and the barrier at the interface ZnO NRs

DOI: 10.1021/acsami.5b02834
ACS Appl. Mater. Interfaces 2015, 7, 11032−11040

and Gr is Φ_0 (Figure 5a). If the applied V_G is negative, the quasi-Fermi level is imbalanced and moves to the closer valence band of Gr (Figure 5b). Consequently, the barrier (Φ_1) between ZnO NRs and Gr is larger ($\Phi_1 > \Phi_0$) and the photogenerated electrons have difficulty drifting from ZnO NRs to Gr, resulting in a low response. When V_G becomes zero in this region, the barrier is narrower and the response increases. In contrast, if a positive V_G is applied, the quasi-Fermi level approaches closer to the conduction band of Gr, and the barrier (Φ_2) between ZnO NRs and Gr is smaller ($\Phi_2 < \Phi_0$) (Figure 5c), leading to enhanced transfer of electrons from ZnO NRs to Gr and an increased response. However, the electric field caused by a positive V_G results in drift of electrons to the gate electrode forming a leakage current. At low gate bias, the leakage current is negligible, but the larger leakage current at a high gate voltage decreases the response. This explains why the response decreases at V_G = 5 V in Figure 2e.

Another important parameter of a photodetector is wavelength selectivity, defined as the wavelength of the optical light where the maximum photoresponse is obtained.[51] To demonstrate the excellent selectivity, the spectral photoresponse of the flexible ZnO NRs/Gr hybrid FET phototransistor for a bias of 1 V at different wavelengths is investigated in Figure 6a, as well as Figure S5 in the Supporting Information. It can be seen that the maximum response is observed at a wavelength of ∼365 nm, while the very small response in the visible region can be neglected. This observation is related to the band-edge absorption, followed by generation of charge carriers.[48] Indeed, only optical light with a higher excited energy than the bandgap of ZnO NRs (3.37 eV)[12,13,52] is able to generate electron−hole pairs to form a photocurrent. For UV light, the incident photons have enough energy to elevate electrons from the valence band to the conduction band to transfer to the Gr channel.[35,39] Besides, the highest photoabsorption of ZnO NRs was observed at a wavelength of ∼365 nm.[35,39,48] These features explain why the device exhibited a high response in the UV light range and reached a peak in response at ∼365 nm. Regarding the visible region, the photon energy was insufficient to generate electron−hole pairs,[35,39] compared with the UV response; hence, the visible response was too small to be observed, as seen in Figure 6a.

In order to study the electrical behaviors of the mechanically bent flexible phototransistor, the UV responsivity was investigated under compressive and tensile bending with varied strain. Figure 6b compares the UV responsivity at the same intensity of UV under straining from compressive to unbent to tensile situations. Under UV irradiance of 0.48 mW cm^{-2}, the deflected phototransistor showed high responsivity and near-invariance of the electrical response under flexure. The almost-unchanged responsivity was ascribed to the lack of significant change in electrical contact at the interface between adjacent ZnO NRs and ZnO NRs/Gr and lack of mechanical deformation of free-standing ZnO NRs on the device channel, instead of mechanical deformation within the body of ZnO NRs.[18]

In addition, to evaluate the reliability and electrical performance of the flexible UV photodetector, the UV response of the device was investigated after cyclic bending of the device. Figure 6c presents the photoresponse of the flexible UV photodetector before and after bending to a strain of 0.5% with various bending cycles under 365 nm UV light exposure. The photoresponse values at 1 mW cm^{-2} UV light intensity were inferred from the fitted response curves (Figure S6 in the Supporting Information). The results indicate that the response characteristics of the flexible photodetector for UV are virtually unchanged (fluctuation of ∼11.5% after 500, 1000, 3000, 5000, and 10 000 bending cycles). Therefore, it can be presumed that the ZnO NRs/Gr hybrid photodetector exhibits high endurance and stability after cyclic bending for practical applications.

CONCLUSION

In summary, the work presented here describes the successful fabrication of a flexible ultraviolet (UV) photodetector based on a hybrid field-effect transistor (FET) structure composed of ZnO nanorods and graphene (ZnO NRs/Gr). The high selectivity of the flexible phototransistor device was demonstrated with a maximum response observed at a wavelength of ∼365 nm. From the negative shift of the Dirac point, the UV sensing mechanism of the device was attributed to the transfer of electrons from ZnO NRs to Gr with a transferred electron concentration per unit of UV intensity of 6×10^{12} electrons per mW cm^{-2}. Under 365 nm wavelength exposure and with a transistor structure, our device exhibited higher photocurrent responsivity and photoconductive gain at a positive gate bias than it did at a negative gate voltage, with maximum values of 2.5×10^6 A W^{-1} and 8.3×10^6, respectively, at a gate bias of 5 V. Interestingly, the responsivity of the flexible UV photodetector was almost entirely unaffected under mechanical deflection. The endurable response of the flexible ZnO NRs/Gr hybrid FET photodetector remained stable after 10 000 cycles of bending. These results suggest high flexibility, long-term electrical stability, and reproducibility, and they also indicate that the flexible UV phototransistor would be acceptable for application in wearable electronics.

METHODS

Fabrication of the Flexible Graphene Field-Effect Transistor (GFET). The architecture of the FET photodetector device is presented in Figure 1a. First, a bottom-gated GFET structure was fabricated. After cleaning the PI substrate with acetone, ethanol, and deionized (DI) water, a thin film of PVP was spin-coated onto the substrate to reduce the roughness of the surface. Next, a 60 nm Ni gate electrode was deposited onto the PI substrate through a shadow mask by e-beam evaporation. To fabricate the ZnO NRs/Gr hybrid FET structure on a flexible device, we optimized many process parameters, including, in particular, the formation of flexible gate dielectric. Here, the sandwich structure of PVP between two layers of 20-nm-thick Al_2O_3 was used as a gate dielectric in which the Al_2O_3 layers were deposited by atomic layer deposition (ALD) at 200 °C, and 400-nm-thick PVP was spin-coated onto the first Al_2O_3 layer. The second Al_2O_3 layer provided a hydrophilic surface for convenient transfer of Gr onto the device. A single layer of Gr was synthesized on a copper foil 75 μm thick, using a chemical vapor deposition (CVD) method.[53,54] The synthesized high-quality Gr was transferred to the target substrate via a gold (Au) transfer process.[41,55,56] In the Au transfer method, 20 nm of Au was deposited onto the Gr film grown on copper foil. The Cu catalyst layer was etched with a $FeCl_3$ solution, and the Gr film supported by the Au layer was then transferred onto the device. The Au layer was completely removed by using a wet etching process (KI/I_2 solution) to avoid impacts of the residue on the device performance.[55,56] Cr/Au (5 nm/50 nm) as the source and drain electrodes were deposited on the Gr layer with a shadow mask by thermal evaporation. The channel length of the device was in the range of 80−110 μm, and its width was 600 μm. Finally, the GFET was dipped into 20% polyethylenimine (PEI) in ethanol solution for 3 h to dope electrons into the Gr channel.[41,57,58]

DOI: 10.1021/acsami.5b02834
ACS Appl. Mater. Interfaces 2015, 7, 11032−11040

Growth of ZnO NRs on the Gr Channel for a Flexible Hybrid Channel FET. Before growing ZnO NRs, source-drain encapsulation (tetratetracontane, TTC) was deposited using a thermal evaporator with a shadow mask to prevent direct contact between ZnO and the electrodes. To obtain high-density ZnO NRs, a 5 wt % dispersion of ZnO nanoparticles (ZnO NPs) was spin-casted onto the Gr channel for 5 min. Notably, the ZnO NPs were modified by oligomeric acidic esters to enhance the adhesion between ZnO NPs and PEI-treated Gr. Finally, ZnO NRs were grown in aqueous solution containing 20 mM zinc nitrate hexahydrate ($Zn(NO)_3{\cdot}6H_2O$), hexamethylenetetramine ($C_6H_{12}N_4$, HMTA) and 200 mL of DI water at 90 °C for 3 h.

Characterization of Flexible Hybrid FET Photodetector. After the growing process, the density of ZnO NRs was checked by field-emission scanning electron microscopy (FE-SEM) (JEOL, Model JSM-6500F). A UV light-emitting diode (LED) was used for exposure during sensor measurement. All electrical and photoresponse characteristics of ZnO NRs/Gr hybrid photodetectors were measured using a semiconductor parameter analyzer (Agilent, Model 4145B) under dark and illuminated conditions. All electrical measurements were carried out in air at room temperature.

■ ASSOCIATED CONTENT

Ⓢ Supporting Information

These materials include the detailed fitting process and the way to calculate the maximum of photovoltage responsivity, photocurrent responsivity and photoconductive gain; the stability; the figure of dependence of photoresponse on UV intensities at different gate bias and on various wavelengths of incident light. The materials are available free of charge via the Internet at The Supporting Information is available free of charge on the ACS Publications website at DOI: 10.1021/acsami.5b02834.

■ AUTHOR INFORMATION

Corresponding Author

*E-mail: nelee@skku.edu.

Notes

The authors declare no competing financial interest.

■ ACKNOWLEDGMENTS

This research was supported by the Basic Science Research Program (No. 2013R1A2A1A01015232) through the National Research Foundation (NRF), funded by the Ministry of Science, ICT & Future Planning.

■ REFERENCES

(1) Nathan, A.; Ahnood, A.; Cole, M. T.; Lee, S.; Suzuki, Y.; Hiralal, P.; Bonaccorso, F.; Hasan, T.; Garcia-Gancedo, L.; Dyadyusha, A.; Haque, S.; Andrew, P.; Hofmann, S.; Moultrie, J.; Chu, D.; Flewitt, A. J.; Ferrari, A. C.; Kelly, M. J.; Robertson, J.; Amaratunga, G. A. J.; Miline, W. Flexible Electronics: The Next Ubiquitous Platform. *Proc. IEEE* **2012**, *100*, 1486−1517.

(2) Stoppa, M.; Chiolerio, A. Wearable Electronics and Smart Textiles: A Critical Review. *Sensors* **2014**, *14*, 11957−11992.

(3) Pang, C.; Lee, C.; Suh, K.-Y. Recent Advances in Flexible Sensors for Wearable and Implantable Devices. *J. Appl. Polym. Sci.* **2013**, *130*, 1429−1441.

(4) Patel, S.; Park, H.; Bonato, P.; Chan, L.; Rodgers, M. A Review of Wearable Sensors and Systems with Application in Rehabilitation. *J. Neuroeng. Rehabil.* **2012**, *9*, 1−17.

(5) Tien, N. T.; Jeon, S.; Kim, D.-I.; Trung, T. Q.; Jang, M.; Hwang, B.-U.; Byun, K.-E.; Bae, J.; Lee, E.; Tok, J. B.-H.; Bao, J.; Lee, N.-E; Park, J.-J. A Flexible Bimodal Sensor Array for Simultaneous Sensing of Pressure and Temperature. *Adv. Mater.* **2014**, *26*, 796−804.

(6) Service, R. F. Inorganic Electronics Begin to Flex Their Muscle. *Science* **2006**, *312*, 1593−1594.

(7) Cima, M. J. Next-Generation Wearable Electronics. *Nat. Biotechnol.* **2014**, *32*, 642−643.

(8) Sun, Y.; Wang, H. H. High-Performance, Flexible Hydrogen Sensors That Use Carbon Nanotubes Decorated with Palladium Nanoparticles. *Adv. Mater.* **2007**, *19*, 2818−2823.

(9) Lochner, C. M.; Khan, Y.; Pierre, A.; Arias, A. C. All-Organic Optoelectronic Sensor for Pulse Oximetry. *Nat. Commun.* **2014**, *5*.

(10) Kim, D.; Shin, G.; Yoon, J.; Jang, D.; Lee, S.-J.; Zi, G.; Ha, J. S. High Performance Stretchable UV Sensor Arrays of SnO_2 Nanowires. *Nanotechnology* **2013**, *24*, 315502.

(11) Chang, S.-P.; Chen, K.-J. Zinc Oxide Nanoparticle Photodetector. *J. Nanomater.* **2012**, *2012*, e602398.

(12) Gedamu, D.; Paulowicz, I.; Kaps, S.; Lupan, O.; Wille, S.; Haidarschin, G.; Mishra, Y. K.; Adelung, R. Rapid Fabrication Technique for Interpenetrated ZnO Nanotetrapod Networks for Fast UV Sensors. *Adv. Mater.* **2014**, *26*, 1541−1550.

(13) Kind, H.; Yan, H.; Messer, B.; Law, M.; Yang, P. Nanowire Ultraviolet Photodetectors and Optical Switches. *Adv. Mater.* **2002**, *14*, 158−160.

(14) Law, J. B. K.; Thong, J. T. L. Simple Fabrication of a ZnO Nanowire Photodetector with a Fast Photoresponse Time. *Appl. Phys. Lett.* **2006**, *88*, 133114.

(15) Shabannia, R.; Hassan, H. A.; Mahmodi, H.; Naderi, N.; Abd, H. R. ZnO Nanorod Ultraviolet Photodetector on Porous Silicon Substrate. *Semicond. Sci. Technol.* **2013**, *28*, 115007.

(16) Zhou, H.; Fang, G.; Liu, N.; Zhao, X. Ultraviolet Photodetectors Based on ZnO Nanorods-Seed Layer Effect and Metal Oxide Modifying Layer Effect. *Nanoscale Res. Lett.* **2011**, *6*, 147.

(17) Liu, N.; Fang, G.; Zeng, W.; Zhou, H.; Cheng, F.; Zheng, Q.; Yuan, L.; Zou, X.; Zhao, X. Direct Growth of Lateral ZnO Nanorod UV Photodetectors with Schottky Contact by a Single-Step Hydrothermal Reaction. *ACS Appl. Mater. Interfaces* **2010**, *2*, 1973−1979.

(18) Bai, S.; Wu, W.; Qin, Y.; Cui, N.; Bayerl, D. J.; Wang, X. High-Performance Integrated ZnO Nanowire UV Sensors on Rigid and Flexible Substrates. *Adv. Funct. Mater.* **2011**, *21*, 4464−4469.

(19) Hatch, S. M.; Briscoe, J.; Dunn, S. A Self-Powered ZnO-Nanorod/CuSCN UV Photodetector Exhibiting Rapid Response. *Adv. Mater.* **2013**, *25*, 867−871.

(20) Liu, J.; Lu, R.; Xu, G.; Wu, J.; Thapa, P.; Moore, D. Development of a Seedless Floating Growth Process in Solution for Synthesis of Crystalline ZnO Micro/Nanowire Arrays on Graphene: Towards High-Performance Nanohybrid Ultraviolet Photodetectors. *Adv. Funct. Mater.* **2013**, *23*, 4941−4948.

(21) Dhara, S.; Giri, P. K. Improved Fast Photoresponse from Al Doped ZnO Nanowires Network Decorated with Au Nanoparticles. *Chem. Phys. Lett.* **2012**, *541*, 39−43.

(22) Durham, J. W.; Zhu, Y. Fabrication of Functional Nanowire Devices on Unconventional Substrates Using Strain-Release Assembly. *ACS Appl. Mater. Interfaces* **2012**, *5*, 256−261.

(23) Wu, Z.; Xue, Y.; Wang, H.; Wu, Y.; Yu, H. ZnO nanorods/Pt and ZnO nanorods/Ag Heteronanostructure Arrays with Enhanced Photocatalytic Degradation of Dyes. *RSC Adv.* **2014**, *4*, 59009−59016.

(24) Yao, I.-C.; Tseng, T.-Y.; Lin, P. ZnO Nanorods Grown on Polymer Substrates as UV Photodetectors. *Sens. Actuators, A* **2012**, *178*, 26−31.

(25) Chen, T.-P.; Young, S.-J.; Chang, S.-J.; Hsiao, C.-H.; Hsu, Y.-J. Bending Effects of ZnO Nanorod Metal−Semiconductor−Metal Photodetectors on Flexible Polyimide Substrate. *Nanoscale Res. Lett.* **2012**, *7*, 214.

(26) Gao, P.; Wang, Z. Z.; Liu, K. H.; Xu, Z.; Wang, W. L.; Bai, X. D.; Wang, E. G. Photoconducting Response on Bending of Individual ZnO Nanowires. *J. Mater. Chem.* **2009**, *19*, 1002−1005.

(27) Yan, C.; Wang, J.; Wang, X.; Kang, W.; Cui, M.; Foo, C. Y.; Lee, P. S. An Intrinsically Stretchable Nanowire Photodetector with a Fully Embedded Structure. *Adv. Mater.* **2014**, *26*, 943−950.

(28) Weiss, N. O.; Zhou, H.; Liao, L.; Liu, Y.; Jiang, S.; Huang, Y.; Duan, X. Graphene: An Emerging Electronic Material. *Adv. Mater.* **2012**, *24*, 5782−5825.

DOI: 10.1021/acsami.5b02834
ACS Appl. Mater. Interfaces 2015, 7, 11032−11040

(29) Zhang, Y.; Tan, Y.-W.; Stormer, H. L.; Kim, P. Experimental Observation of the Quantum Hall Effect and Berry's Phase in Graphene. *Nature* **2005**, *438*, 201−204.
(30) Chen, J.-H.; Jang, C.; Xiao, S.; Ishigami, M.; Fuhrer, M. S. Intrinsic and Extrinsic Performance Limits of Graphene Devices on SiO_2. *Nat. Nanotechnol.* **2008**, *3*, 206−209.
(31) Lee, C.; Wei, X.; Kysar, J. W.; Hone, J. Measurement of the Elastic Properties and Intrinsic Strength of Monolayer Graphene. *Science* **2008**, *321*, 385−388.
(32) Choi, W. M.; Shin, K.-S.; Lee, H. S.; Choi, D.; Kim, K.; Shin, H.-J.; Yoon, S.-M.; Choi, J.-Y.; Kim, S.-W. Selective Growth of ZnO Nanorods on SiO_2/Si Substrates Using a Graphene Buffer Layer. *Nano Res.* **2011**, *4*, 440−447.
(33) Wang, H.; Wu, Y.; Cong, C.; Shang, J.; Yu, T. Hysteresis of Electronic Transport in Graphene Transistors. *ACS Nano* **2010**, *4*, 7221−7228.
(34) Dang, V. Q.; Trung, T. Q.; Kim, D.-I.; Duy, L. T.; Hwang, B.-U.; Lee, D.-W.; Kim, B.-Y.; Toan, L. D.; Lee, N.-E. Ultrahigh Responsivity in Graphene−ZnO Nanorod Hybrid UV Photodetector. *Small* **2015**, DOI: 10.1002/smll.201403625.
(35) Nie, B.; Hu, J.-G.; Luo, L.-B.; Xie, C.; Zeng, L.-H.; Lv, P.; Li, F.-Z.; Jie, J.-S.; Feng, M.; Wu, C.-Y.; Yu, Y.-Q.; Yu, S.-H. Monolayer Graphene Film on ZnO Nanorod Array for High-Performance Schottky Junction Ultraviolet Photodetectors. *Small* **2013**, *9*, 2872−2879.
(36) Chang, H.; Sun, Z.; Ho, K. Y.-F.; Tao, X.; Yan, F.; Kwok, W.-M.; Zheng, Z. A Highly Sensitive Ultraviolet Sensor Based on a Facile *In Situ* Solution-Grown ZnO Nanorod/Graphene Heterostructure. *Nanoscale* **2011**, *3*, 258−264.
(37) Zhang, H.; Babichev, A. V.; Jacopin, G.; Lavenus, P.; Julien, F. H.; Egorov, A. Y.; Zhang, J.; Pauporté, T.; Tchernycheva, M. Characterization and Modeling of a ZnO Nanowire Ultraviolet Photodetector with Graphene Transparent Contact. *J. Appl. Phys.* **2013**, *114*, 234505.
(38) Chen, T. P.; Young, S.-J.; Chang, S.-J.; Hsiao, C. H.; Wu, S. L. Photoelectrical and Low-Frequency Noise Characteristics of ZnO Nanorod Photodetectors Prepared on Flexible Substrate. *IEEE Trans. Electron Devices* **2013**, *60*, 229−234.
(39) Shao, D.; Yu, M.; Sun, H.; Hu, T.; Lian, J.; Sawyer, S. High Responsivity, Fast Ultraviolet Photodetector Fabricated from ZnO Nanoparticle−Graphene Core−Shell Structures. *Nanoscale* **2013**, *5*, 3664−3667.
(40) Choi, D.; Choi, M.-Y.; Choi, W. M.; Shin, H.-J.; Park, H.-K.; Seo, J.-S.; Park, J.; Yoon, S.-M.; Chae, S. J.; Lee, Y. H.; Kim, S.-W.; Choi, J.-Y.; Lee, S. Y.; Kim, J. M. Fully Rollable Transparent Nanogenerators Based on Graphene Electrodes. *Adv. Mater.* **2010**, *22*, 2187−2192.
(41) Dang, V. Q.; Kim, D.-I.; Duy, L. T.; Kim, B.-Y.; Hwang, B.-U.; Jang, M.; Shin, K.-S.; Kim, S.-W.; Lee, N.-E. Piezoelectric Coupling in a Field-Effect Transistor with a Nanohybrid Channel of ZnO Nanorods Grown Vertically on Graphene. *Nanoscale* **2014**, *6*, 15144−15150.
(42) Tan, Y.-W.; Zhang, Y.; Bolotin, K.; Zhao, Y.; Adam, S.; Hwang, E. H.; Das Sarma, S.; Stormer, H. L.; Kim, P. Measurement of Scattering Rate and Minimum Conductivity in Graphene. *Phys. Rev. Lett.* **2007**, *99*, 246803.
(43) Yan, J.; Fuhrer, M. S. Correlated Charged Impurity Scattering in Graphene. *Phys. Rev. Lett.* **2011**, *107*, 206601.
(44) Li, J.; Niu, L.; Zheng, Z.; Yan, F. Photosensitive Graphene Transistors. *Adv. Mater.* **2014**, *26*, 5239−5273.
(45) Jun, J. H.; Seong, H.; Cho, K.; Moon, B.-M.; Kim, S. Ultraviolet Photodetectors Based on ZnO Nanoparticles. *Ceram. Int.* **2009**, *35*, 2797−2801.
(46) Soci, C.; Zhang, A.; Xiang, B.; Dayeh, S. A.; Aplin, D. P. R.; Park, J.; Bao, X. Y.; Lo, Y. H.; Wang, D. ZnO Nanowire UV Photodetectors with High Internal Gain. *Nano Lett.* **2007**, *7*, 1003−1009.
(47) Guo, W.; Xu, S.; Wu, Z.; Wang, N.; Loy, M. M. T.; Du, S. Oxygen-Assisted Charge Transfer Between ZnO Quantum Dots and Graphene. *Small* **2013**, *9*, 3031−3036.
(48) Dhara, S.; Giri, P. K. Enhanced UV Photosensitivity from Rapid Thermal Annealed Vertically Aligned ZnO Nanowires. *Nanoscale Res. Lett.* **2011**, *6*, 1−8.
(49) Manekkathodi, A.; Lu, M.-Y.; Wang, C. W.; Chen, L.-J. Direct Growth of Aligned Zinc Oxide Nanorods on Paper Substrates for Low-Cost Flexible Electronics. *Adv. Mater.* **2010**, *22*, 4059−4063.
(50) Zhai, T.; Li, L.; Wang, X.; Fang, X.; Bando, Y.; Golberg, D. Recent Developments in One-Dimensional Inorganic Nanostructures for Photodetectors. *Adv. Funct. Mater.* **2010**, *20*, 4233−4248.
(51) Dahara, S.; Giri, P. K. ZnO Nanowire Heterostructures: Intriguing Photophysics and Emerging Applications. *Rev. Nanosci. Nanotechnol.* **2013**, *2*, 147−170.
(52) Lin, S.; Tang, H.; Ye, Z.; He, H.; Zeng, Y.; Zhao, B.; Zhu, L. Synthesis of Vertically Aligned Al-Doped ZnO Nanorods Array with Controllable Al Concentration. *Mater. Lett.* **2008**, *62*, 603−606.
(53) Kim, K. S.; Zhao, Y.; Jang, H.; Lee, S. Y.; Kim, J. M.; Kim, K. S.; Ahn, J.-H.; Kim, P.; Choi, J.-Y.; Hong, B. H. Large-Scale Pattern Growth of Graphene Films for Stretchable Transparent Electrodes. *Nature* **2009**, *457*, 706−710.
(54) Reina, A.; Jia, X.; Ho, J.; Nezich, D.; Son, H.; Bulovic, V.; Dresselhaus, M. S.; Kong, J. Large Area, Few-Layer Graphene Films on Arbitrary Substrates by Chemical Vapor Deposition. *Nano Lett.* **2008**, *9*, 30−35.
(55) Jang, M.; Trung, T. Q.; Jung, J.-H.; Kim, B.-Y.; Lee, N.-E. Improved Performance and Stability of Field-Effect Transistors with Polymeric Residue-Free Graphene Channel Transferred by Gold Layer. *Phys. Chem. Chem. Phys.* **2014**, *16*, 4098−4105.
(56) Jung, J. H.; Sohn, I. Y.; Kim, D. J.; Kim, B. Y.; Jang, M.; Lee, N.-E. Enhancement of Protein Detection Performance in Field-Effect Transistors with Polymer Residue-Free Graphene Channel. *Carbon* **2013**, *62*, 312−321.
(57) Farmer, D. B.; Golizadeh-Mojarad, R.; Perebeinos, V.; Lin, Y.-M.; Tulevski, G. S.; Tsang, J. C.; Avouris, P. Chemical Doping and Electron−Hole Conduction Asymmetry in Graphene Devices. *Nano Lett.* **2009**, *9*, 388−392.
(58) Liu, H.; Liu, Y.; Zhu, D. Chemical Doping of Graphene. *J. Mater. Chem.* **2011**, *21*, 3335−3345.
(59) Yang, Q.; Guo, X.; Wang, W.; Zhang, Y.; Xu, S.; Lien, D. H.; Wang, Z. L. Enhancing Sensitivity of a Single ZnO Micro-/Nanowire Photodetector by Piezo-Phototronic Effect. *ACS Nano* **2010**, *4*, 6285−6291.
(60) Um, H.-D.; Moiz, S. A.; Park, K.-T.; Jung, J.-Y.; Jee, S.-W.; Ahn, C. H.; Kim, D. C.; Cho, H. K.; Kim, D.-W.; Lee, J.-H. Highly Selective Spectral Response with Enhanced Responsivity of *n*-ZnO/*p*-Si Radial Heterojunction Nanowire Photodiodes. *Appl. Phys. Lett.* **2011**, *98*, 033102.
(61) Yang, Z.; Wang, M.; Song, X.; Yan, G.; Ding, Y.; Bai, J. High-Performance ZnO/Ag Nanowire/ZnO Composite Film UV Photodetectors with Large Area and Low Operating Voltage. *J. Mater. Chem. C* **2014**, *2*, 4312−4319.

DOI: 10.1021/acsami.5b02834
ACS Appl. Mater. Interfaces 2015, 7, 11032−11040